Studies of Nylon 6 / PET Polymer Blends: Structure and Some Physical Properties

D. S. VARMA and V. K. DHAR, *Textile Technology Department, Indian Institute of Technology, Delhi, New Delhi-110 016, India*

Synopsis

The structure, morphology, and some physical properties of nylon 6/polyethylene terephthalate (PET) blends (PET varying from 10 to 50%) have been reported here. Various techniques such as SEM, X-ray diffraction, birefringence, density, DTA, and DSC have been used. SEM studies revealed that in the blend PET is dispersed as spheres in the nylon 6 matrix. On melt spinning these are elongated in the form of rods and a fibril matrix-type morphology is developed. PET reinforces the (202, 002) lattice planes of nylon 6 up to a certain composition, resulting in increased crystallinity. Both nylon 6 and PET aid each other in mutual nucleation. The highly oriented and extended PET chains hold the nylon 6 molecular chains along their length resulting in increased orientation of the blend fiber system. All these studies further revealed that the improvement in some of the observed properties is due to the fibril-reinforced morphology and the crystallization behavior of the two components, especially that of nylon 6 in the presence of PET.

INTRODUCTION

In this paper an attempt is made at characterizing the structure and state of dispersion of polyethylene terephthalate (PET) in the nylon 6/PET blend system. Since both nylon 6 and PET components are crystalline polymers, it is therefore essential to examine in addition to the morphology, the crystalline structure of the blend and how it influences the properties of nylon 6/PET polymer blend. The various techniques used to study the system were (i) scanning electron microscopy (SEM), (ii), X-ray diffraction, (iii) optical birefringence, (iv) density, (v) differential thermal analysis (DTA), and (vi) differential scanning calorimetry (DSC).

EXPERIMENTAL

The polymer chips of nylon 6 ($[\eta] = 0.57$) and PET ($[\eta] = 0.69$) were tumble mixed in various proportions. The melt blending of the dried polymer chips was carried out on a single-screw extrusion machine using the following parameters: screw speed 20 rpm, temperature of zones 1, 2, 3, and the die zone 240, 250, 260, and 260°C, respectively; diameter of the die orifice 3 mm. Melt rheology studies were carried out on an MCR capillary rheometer installed on an Instron tester. The rheometer extrudates emerging at 270°C were collected and examined.

Melt spinning of nylon 6, PET, and nylon 6/PET blend chips was carried out on a laboratory melt-spinning unit. The spinning of nylon 6 was done at 240°C and that of PET and nylon 6/PET blends at 270°C. All the fibers

Journal of Applied Polymer Science, Vol. 33, 1103–1124 (1987)
 CCC 0021-8995/87/041103-22$04.00

were drawn at 125°C to a draw ratio of 5, on a bench scale drawing apparatus. The drawn fibers were heat set at 140°C for one hr in an air oven.

Scanning electron microscopy (SEM) studies were carried out on a Cambridge Stereoscan Model S4-10 instrument. The samples were mounted on special stubs and gold coated for a coating thickness of about 200 Å. Longitudinal and cross-sectional views of the samples were examined.

Etching of the rheometer extrudate rods was done with dilute formic acid (58% by volume). Etching time of 2–5 min was given. The fibers were then gently washed in distilled water, allowed to dry, and then mounted on the sample holder for examination.

Wide-angle X-ray diffraction patterns were recorded on a Norelco X-ray diffraction unit, employing copper K_α radiation, at 30 kV, 20 mA, and a sample to film distance of 4 cm. Exposure time, film developing, fixing, and washing times were kept the same in every case.

For crystallite orientation measurements the filaments were wound on an aluminum frame to give a bunch of parallel fibers (about 1.5 mm broad). The frame was then mounted on the sample holder so that the fibers were perpendicular to the path of the X-ray beam. An equal number of filaments were wound in each case.

To obtain powder patterns, the fibers were cut into very small powder of approximately 50 mesh. Equal weights of the powdered samples in every case were then pressed into a pellet of about 1 mm thickness with the help of a hydraulic press. The pellet was fixed with an adhesive on the aluminum frame and placed in the path of the X-ray beam.

The X-ray diffraction photographs of the samples were scanned on a Joyce Loebl MKIIIS Ratio Recording Microdensitometer.

Powder patterns of the fiber samples were scanned radially and the intensity vs. 2θ scans obtained. The "d" spacings corresponding to the various reflections were obtained using the Bragg relation $2d \sin\theta = n\lambda$, where λ is the wavelength of the X-rays used and n is the order of reflection. The value of λ used was 1.5418 Å and n was taken as unity.

For studying the crystallite orientation in the fiber samples, azimuthal scans (I vs. ϕ) of the important reflections on the fiber photographs were obtained. For this purpose, Polar Table Attachment was used. The Herman's orientation factor (f_c) was obtained from the relation:[1]

$$f_c = \tfrac{1}{2}(3\langle\cos^2\phi\rangle - 1)$$

where $\langle\cos^2\phi\rangle$ is the mean square cosine (averaged over all the crystallites) of the angle between a given crystal axis and the fiber axis. Thus

$$\langle\cos^2\phi\rangle = \frac{\sum_{\phi=0}^{\phi=\phi_1} I(\phi)\sin\phi\cos^2\phi}{\sum_{\phi=0}^{\phi=\phi_1} I(\phi)\sin\phi}$$

where ϕ_1 is the value of the azimuthal angle (ϕ) at the position where $I = 0$. An appropriate baseline for the I vs. ϕ plot was drawn. The azimuthal

intensity values were measured at intervals of $\phi = 0.57°$ from the maximum to the minimum intensity values. The summations in the numerator and denominator of the above equation were evaluated. The value of $\langle \cos^2\phi \rangle$ thus obtained was used to get the Herman's orientation factor (f_c).

Birefringence of the fiber samples was measured with the help of a Berek compensator used with a polarizing microscope.

Density measurements were made with a 6-column density measuring apparatus (Davenport Ltd, England). Carbon tetrachloride and xylene were used to prepare the columns.

DTA and DSC studies were carried out with the help of Stanton Redcroft Model 671 and Perkin Elmer DSC 1B instruments, respectively. The heats of fusion of nylon 6 component in the blend fibers were measured from the DTA traces.[2] These values of the heats of fusion were normalized to 100% nylon 6 content and then were used to find the percent crystallinity of the nylon 6 component in the blend fibers.[3,4]

RESULTS

The scanning electron micrographs of the cross-sectional views of chips show PET in the blends in the form of spherical inclusions; the spheres sitting in the holes of the nylon 6 matrix (Fig. 1). The sizes of the spheres ranged between 1.25 to 4 μm. The micrographs of the capillary rheometer extrudates treated with formic acid are shown in Fig. 2. At lower shear rates, PET is in the form of elongated spheres while at higher shear rates it is seen in the form of rods.

The X-ray diffraction photographs of the fibers are shown in Fig. 3. From the microdensitometer traces of powder X-ray diffraction photographs of the fibers (Fig. 4) it is seen that blending PET into nylon 6 does not result in any shift in the peak positions of either (200) or the (202, 002) reflections. However, the reflection due to the (202, 002) planes is seen to increase in intensity up to the 70/30 nylon 6/PET composition. On blending PET into nylon 6, the Herman's crystallite orientation factor for the (202, 002) planes of nylon 6 (Fig. 5) increases abruptly for 10% PET. There is a slight increase with further additions of PET up to 70/30 nylon 6/PET composition after which it starts decreasing becoming quite low for the 50/50 nylon 6/PET composition than that for pure nylon 6. Similar results are obtained for optical birefringence data also (Fig. 6).

The density of the nylon 6 fiber is seen to increase linearly with the increase in the PET content up to the 50/50 nylon 6/PET composition (Fig. 7).

From the DTA and DSC traces of fibers [Fig. 8 (a), (b)] it is seen that only the fusion peaks have registered, with nylon 6 and PET showing their characteristic peaks at the respective melting points. The DSC of as-spun blend fibers and PET fiber (Fig. 9) showed a glass transition peak/baseline shift around 70°C and a crystallization exotherm. The glass transition and crystallization peaks/baseline shifts are not observed in nylon 6. The crystallization peaks occur around 116°C for the blends and around 136°C for PET. The heat of fusion increases with the increase in the PET content up to 70/30 nylon 6/PET composition. With further increase in the PET content it is found to decrease. The heat of fusion crystallinity plot is given in Fig. 10.

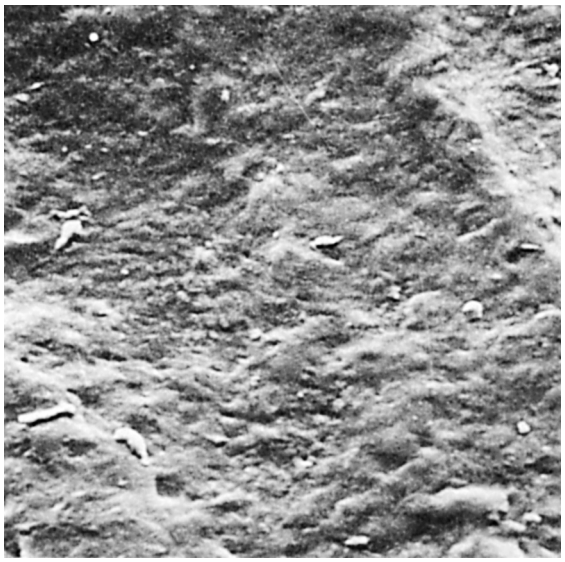

(a)

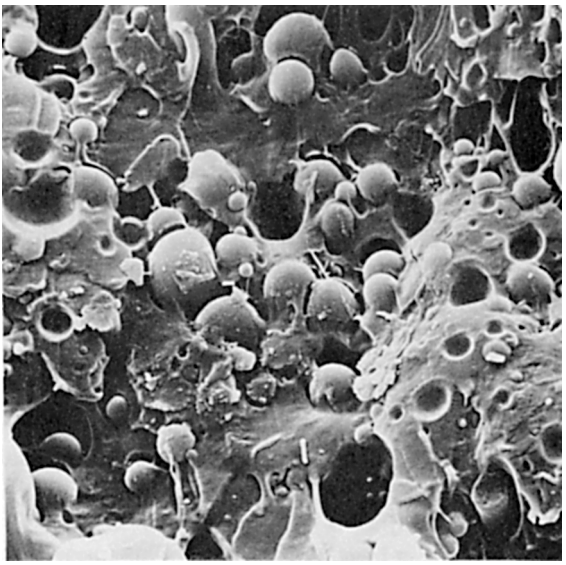

(b)

Fig. 1. SEMs of cross-sectional views of nylon 6 and N6/PET blend chips. (a) Nylon 6 × 1700, (b) 90/10 N6/PET × 1680, (c) 80/20 N6/PET × 1260, (d) 70/30 N6/PET × 1260, (e) 50/50 N6/PET × 1680.

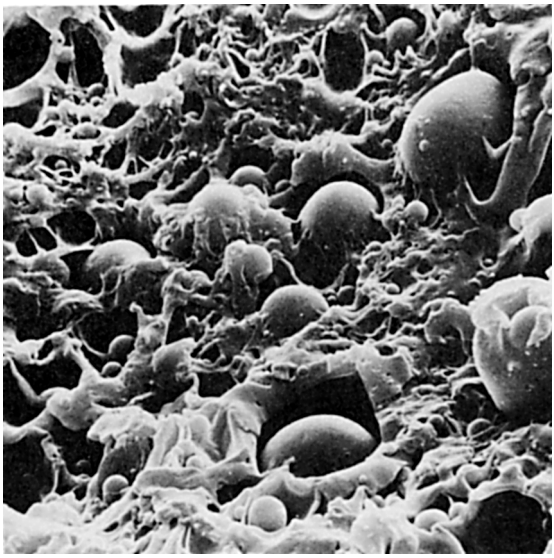

(c)

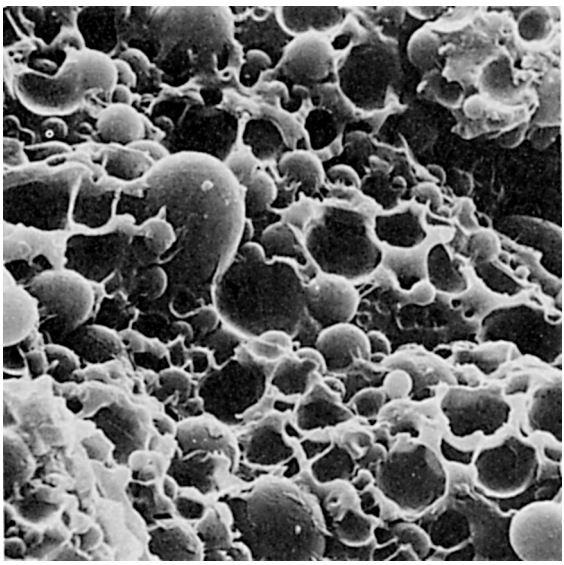

(d)

Fig. 1. (*Continued from the previous page.*)

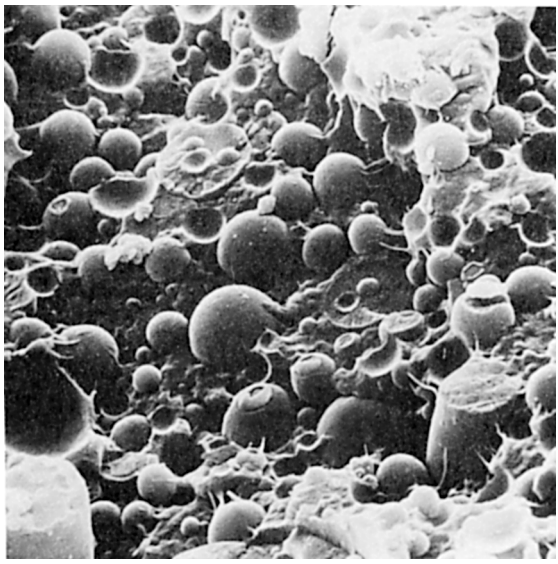

(e)

Fig. 1. (*Continued from the previous page.*)

DISCUSSION

The SEM studies of blend chips and capillary rheometer extrudates were carried out instead of the blend fiber because the blend morphology could not be examined in fibers. However, the morphology developed when the polymer is forced out through the rheometer capillary die can be thought of as approximating the morphology/state of dispersion developed during spinning. Therefore, the rheometer extrudates which came out of the die in the form of thick filaments were studied.

In the blend chips PET is seen to be dispersed in nylon 6 in the form of spheres (Fig. 1). In the case of formic acid-etched rheometer extrudates (70/30, 60/40, and 50/50 nylon 6/PET blends) PET is dispersed in nylon 6 matrix at low shear rate (58 s^{-1}) as elongated spheres, and at higher shear rates as rods aligned sufficiently parallel to each other (Fig. 2). It can be argued that when the PET rods in the blend (which are already aligned sufficiently parallel to each other at higher shear rates) are drawn, a fibril matrix type of morphology is expected with PET fibrils in the form of adjacent layers in the nylon 6 base.

Since the level of heterogeneity of PET in the blends was found to be more than 1.25 μm, it follows that nylon 6/PET blend is an incompatible system. This is because when the particle size of the dispersed phase is larger than the wavelength of visible light the blend system is phase separated and hence incompatible.[5]

In the X-ray diffraction pattern, the absence of any shift in the positions of principal reflections shows that the crystalline lattice of nylon 6 is not affected by blending PET into it. Furthermore, the change in the intensity of reflection

(a, i)

(a, ii)

Fig. 2. SEMs of formic acid etched capillary rheometer extrudates at various shear rates: longitudinal views. (a) 70/30 N6/PET, (i) Shear rate $5.8 \times 10\ s^{-1} \times 3500$, (ii) Shear rate $2.9 \times 10^2 s^{-1} \times 3300$; (b) 60/40 N6/PET, (i) $5.8 \times 10\ s^{-1} \times 7700$, (ii) $1.15 \times 10^2\ s^{-1} \times 1500$, (iii) $2.9 \times 10^2\ s^{-1} \times 800$, (c) 50/50 N6/PET, (i) $5.8 \times 10\ s^{-1} \times 7000$, (ii) $1.15 \times 10^2\ s^{-1} \times 3500$, (iii) $2.9 \times 10^2\ s^{-1} \times 800$, (iv) $5.8 \times 10^2\ s^{-1} \times 1600$.

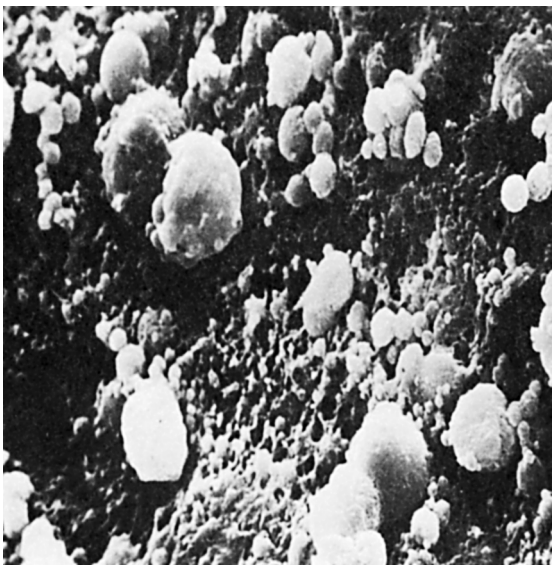

(b, i)

(b, ii)

Fig. 2. (*Continued from the previous page.*)

due to (202, 002) planes suggests that PET reinforces the (202, 002) lattice planes of nylon 6 fiber. These reinforced lattice planes may be responsible for increased crystallinity of nylon 6 up to the 70/30 nylon 6/PET composition. For the 60/40 and 50/50 nylon 6/PET compositions the lattice planes are not reinforced. This may be giving rise to lower crystallinity. Thus a PET content

(b, iii)

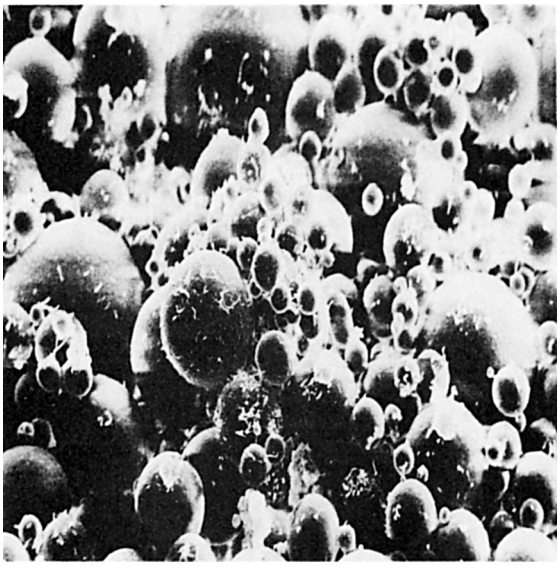

(c, i)

Fig. 2. (*Continued from the previous page.*)

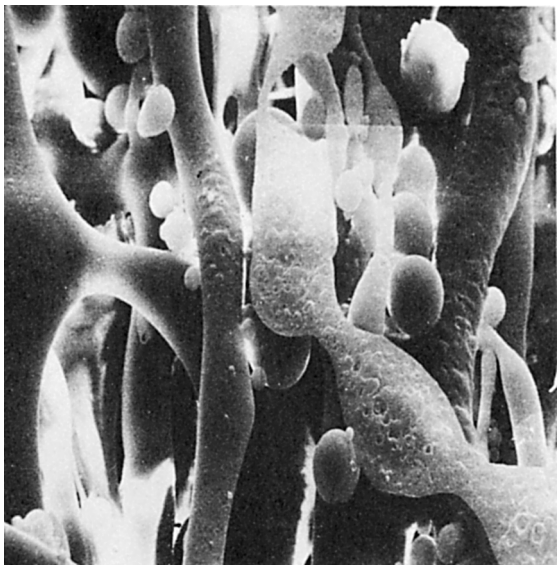

(c, ii)

(c, iii)

Fig. 2. (*Continued from the previous page.*)

(c, iv)

Fig. 2. (*Continued from the previous page.*)

of 30% may be the optimum amount that can lead to maximum crystallization of nylon 6. When the PET content becomes comparable to nylon 6 the (010) and (100) reflections due to PET are manifested in the diffraction pattern (Figure 4).

The increase in the crystallite orientation up to 70/30 nylon 6/PET fiber composition may be due to the drawn PET fibrils acting as boundary layers to the nylon 6 crystallites oriented in the fiber direction. The drawn PET fibrils consist of highly oriented crystallites. When the PET content exceeds 30%, the formation of boundary layers may not be to such a large extent. However, the decreased crystallite orientation for the 50/50 nylon 6/PET fiber composition is almost as low as that of pure nylon 6 fiber (Figure 5). In other words, we can say that PET crystallites may be arranging themselves in the intercrystalline regions of nylon 6 in the preferential fiber direction in such a way as to reinforce the crystalline lattice planes (202, 002) of nylon 6, leading to an increase in both the crystallinity and orientation of the blend fiber. A PET content of 30% may be the optimum amount that can go into these intercrystalline domains.

The total orientation of the fibers obtained from birefringence measurements also showed a trend similar to that obtained from the crystallite orientation measurements. Here also after the 70/30 nylon 6/PET composition the birefringence of the blend fiber goes down, but the values are still higher than that of nylon 6. As much as 30–40% PET content is the optimum proportion that could be reinforcing the nylon 6 chains along the fiber axis.

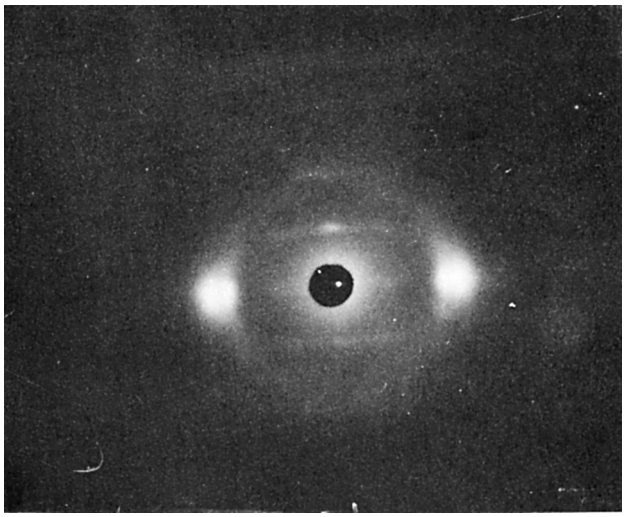

(a)

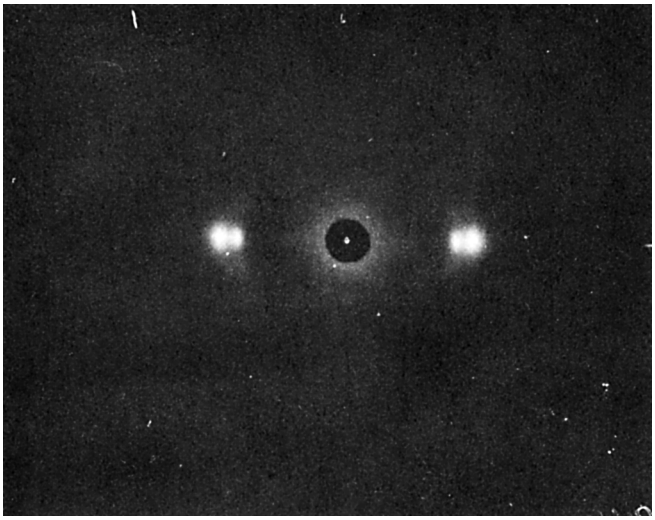

(b)

Fig. 3. X-ray diffraction photographs of nylon 6, PET and blend fibers. (a) Nylon 6, (b) 90/10 N6/PET, (c) 80/20 N6/PET, (d) 70/30 N6/PET, (e) 60/40 N6/PET, (f) 50/50 N6/PET, (g) PET.

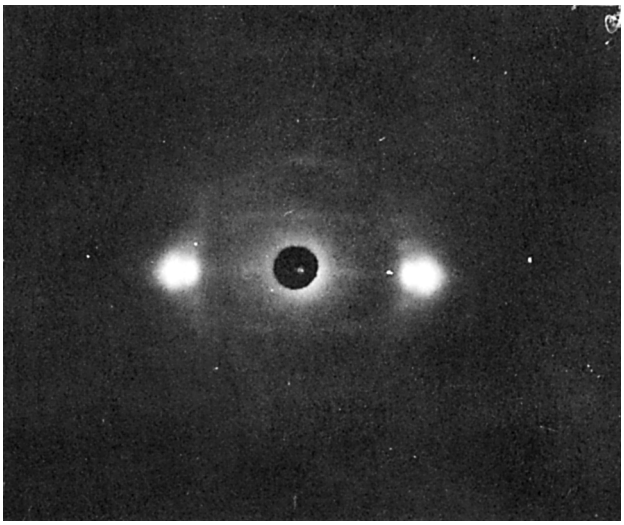

(c)

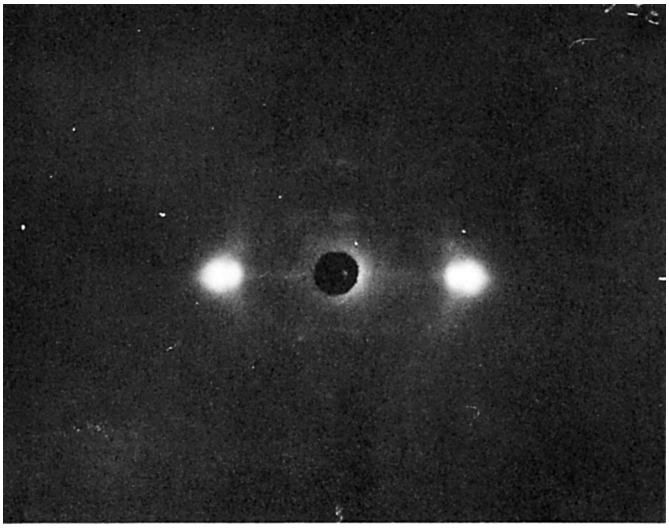

(d)

Fig. 3. (*Continued from the previous page.*)

The form birefringence of the blend fiber samples was calculated using the formula[6]

$$\Delta n_f = \frac{v_1 v_2 (n_1^2 - n_2^2)}{2n_{11}[(v_1 + 1)n_2^2 + v_2 n_1^2]}$$

where v_1 and v_2 are the volume fractions of the dispersed phase (PET) and

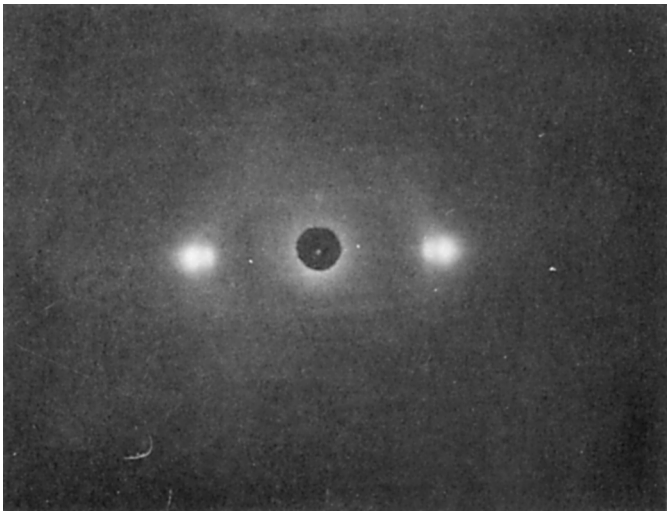

(e)

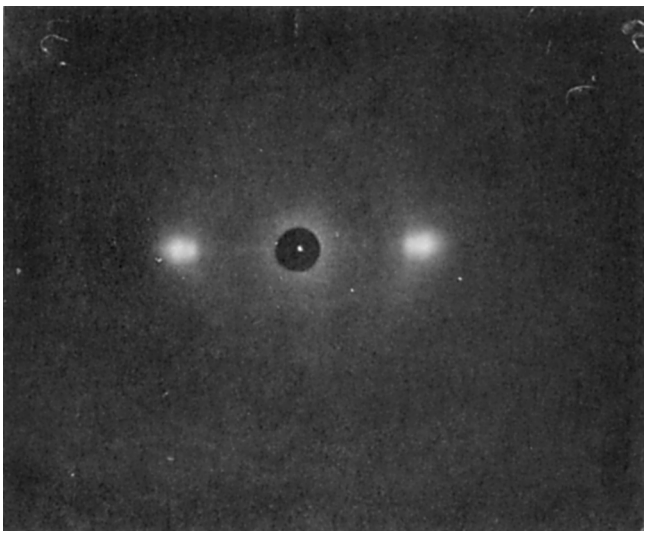

(f)

Fig. 3. *(Continued from the previous page.)*

the surrounding medium (nylon 6), respectively, n_1 and n_2 their corresponding refractive indices. n_{11} refers to the refractive index of the blend composition along the fiber axis. The values of form birefringence obtained are given in Table 1. It can be seen that these values are very small and do not have any effect on the total birefringence of the nylon 6/PET blend fiber system.

The theoretical density of the blend fibers was calculated by assuming an ideal mixture where there is no association between the molecules and the

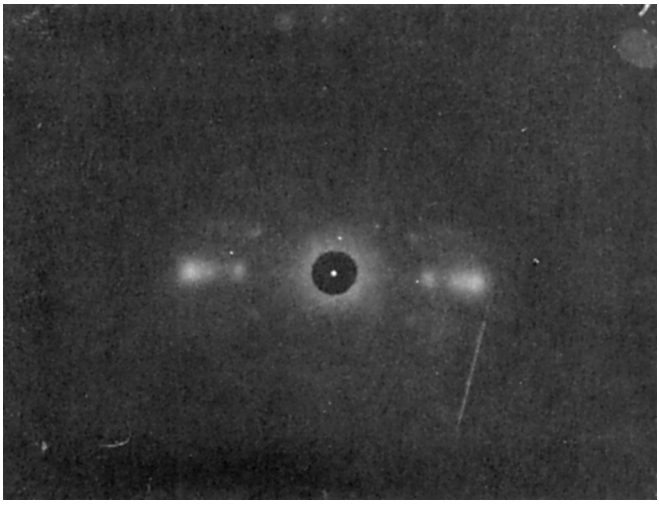

(g)

Fig. 3. *(Continued from the previous page.)*

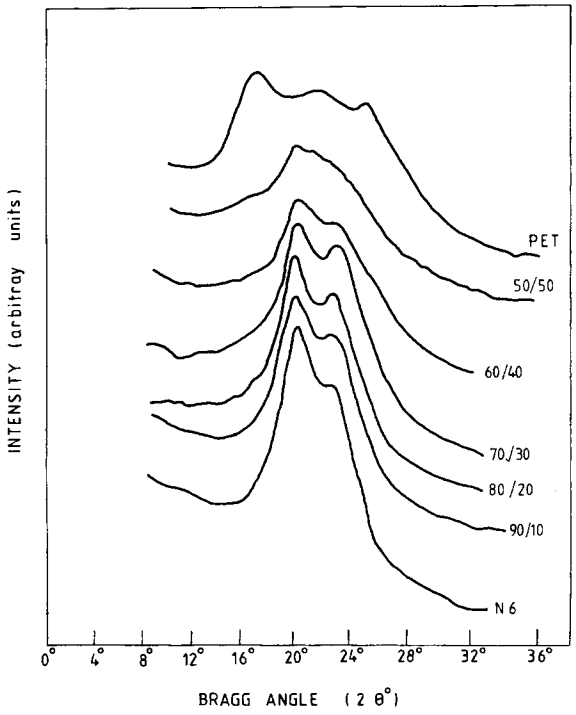

Fig. 4. Microdensitometer traces (I vs. 2θ) of X-ray powder diffraction photographs of nylon 6, PET and nylon 6/PET blend fibers (curves displaced along the ordinate).

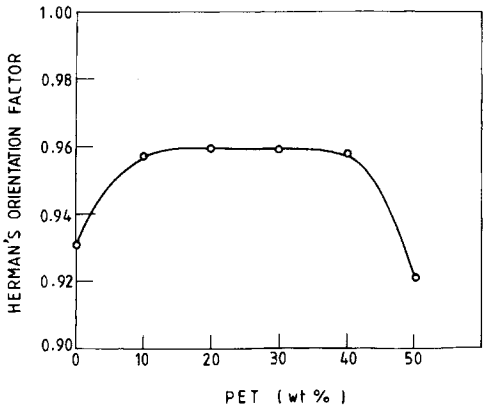

Fig. 5. Composition dependence of Herman's orientation factor for the (202, 002) planes of nylon 6 in nylon 6/PET blend fibers.

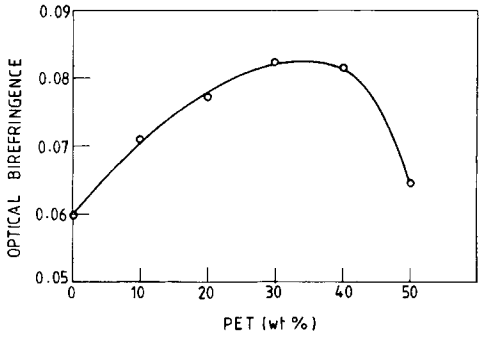

Fig. 6. Composition dependence of optical birefringence in nylon 6/PET blend fibers.

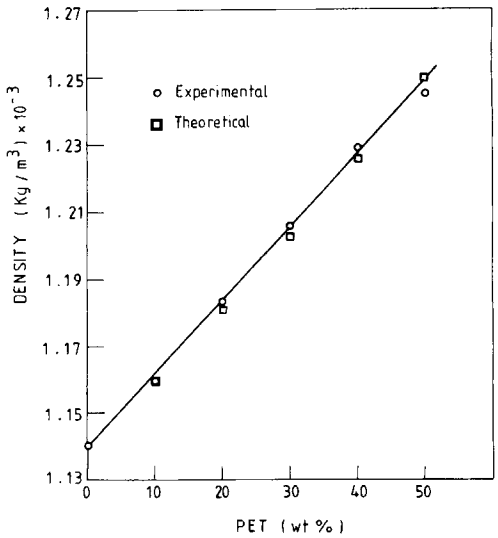

Fig. 7. Composition dependence of density for nylon 6/PET blend fibers.

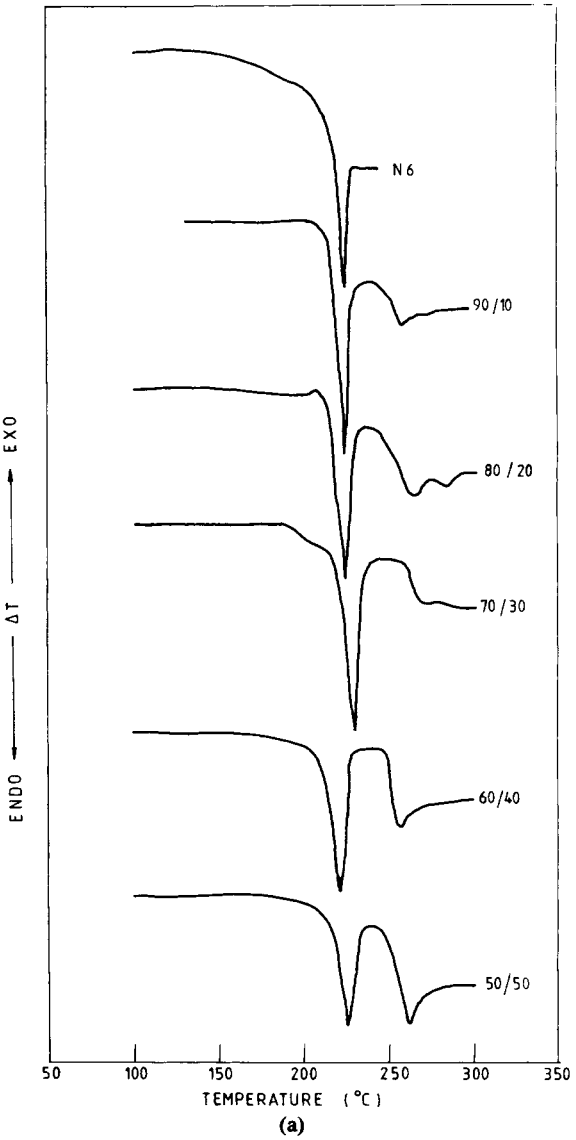

Fig. 8. DTA (a) and DSC (b) traces of drawn nylon 6 and nylon 6/PET blend fibers (curves displaced along the ordinate).

density follows the mixture law.[7]

$$\frac{1}{\rho_{\text{Blend}}} = \frac{w_1}{\rho_{\text{N6}}} + \frac{w_2}{\rho_{\text{PET}}}$$

where w_1 and w_2 are the weight fractions of the blend components nylon 6 and PET, ρ_{N6} and ρ_{PET} their corresponding densities, respectively. The fairly

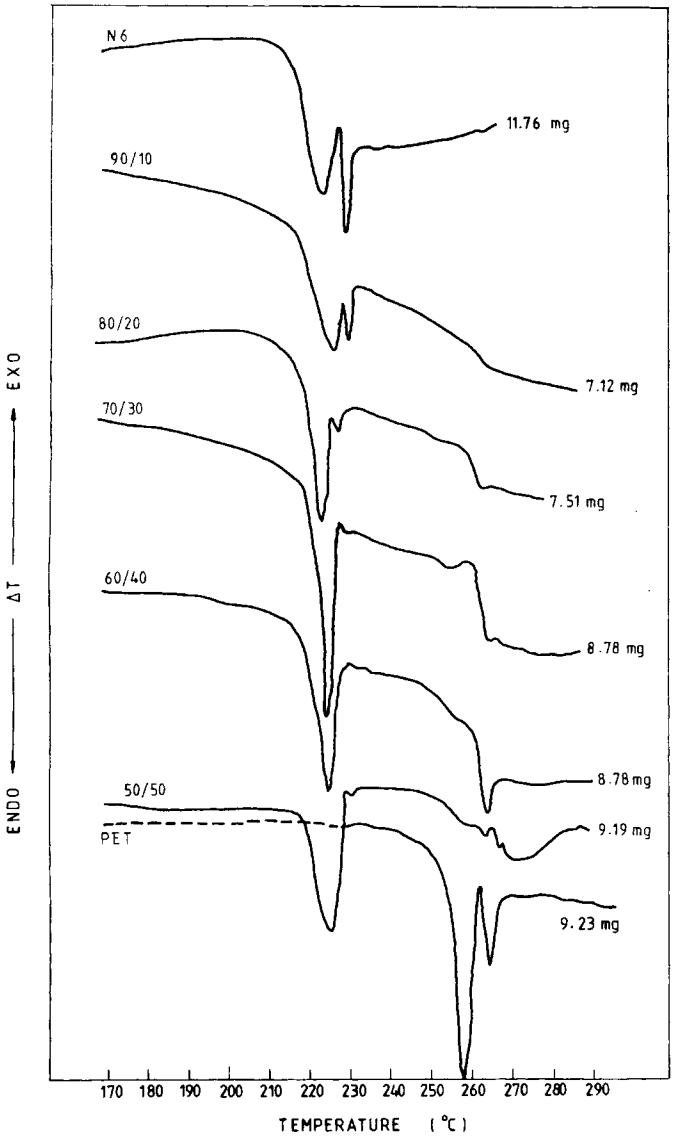

(b)

Fig. 8. (*Continued from the previous page.*)

good agreement between the theoretical and experimental density values suggests that nylon 6/PET is an incompatible system.[8] Furthermore, using the method adopted by Wlochowicz and Jeziorny,[9] the crystallinity of the nylon 6/PET blend fiber system was calculated by the following relations:

$$\frac{1}{\rho^{(C)}_{\text{Blend}}} = \frac{w_1}{\rho^{(C)}_{\text{N6}}} + \frac{w_2}{\rho^{(C)}_{\text{PET}}}$$

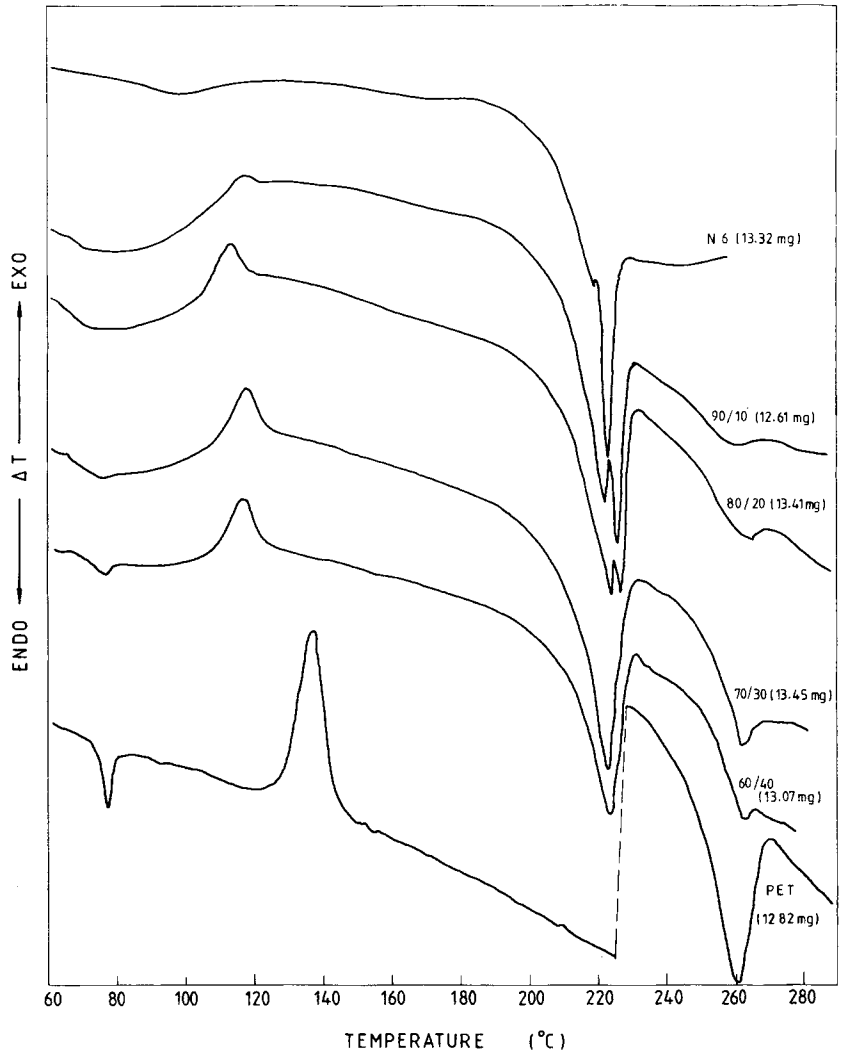

Fig. 9. DSC traces of as-spun nylon 6, PET and nylon 6/PET blend fibers (curves displaced along the ordinate).

and

$$\frac{1}{\rho^{(A)}_{\text{Blend}}} = \frac{w_1}{\rho^{(A)}_{\text{N6}}} + \frac{w_2}{\rho^{(A)}_{\text{PET}}}$$

$\rho^{(C)}_{\text{N6}}$ = Density of the totally crystalline nylon 6 fiber
$\rho^{(A)}_{\text{N6}}$ = Density of the totally amorphous nylon 6 fiber
$\rho^{(C)}_{\text{PET}}$ = Density of the totally crystalline PET fiber
$\rho^{(A)}_{\text{PET}}$ = Density of the totally amorphous PET fiber

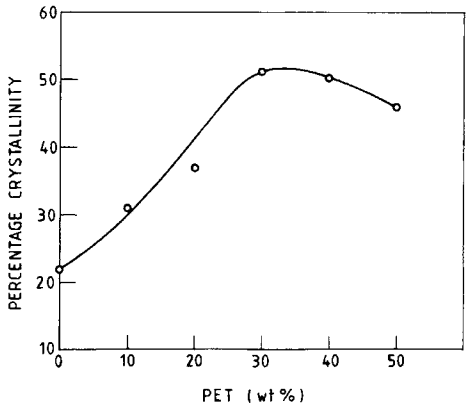

Fig. 10. Composition dependence of nylon 6 crystallinity (from heat of fusion measurements) in nylon 6/PET blend fibers.

TABLE I
Form Birefringence of Blend Fiber Samples

Polymer composition	Form birefringence
90/10 N6/PET	0.0002
80/20 N6/PET	0.0004
70/30 N6/PET	0.0005
60/40 N6/PET	0.0006
50/50 N6/PET	0.0006

$\rho^{(C)}_{Blend}$ and $\rho^{(A)}_{Blend}$ are the densities of the blend of definite proportions of nylon 6 and PET in the definite crystalline and amorphous states, respectively. The following values were used:[4]

$$\rho^{(C)}_{N6} = 1.21 \times 10^3 \text{ kg/m}^3 \qquad \rho^{(C)}_{PET} = 1.455 \times 10^3 \text{ kg/m}^3$$

$$\rho^{(A)}_{N6} = 1.11 \times 10^3 \text{ kg/m}^3 \qquad \rho^{(A)}_{PET} = 1.335 \times 10^3 \text{ kg/m}^3$$

The weight percent crystallinity of the blend fibers was calculated from the density data using the formula[10]

$$\frac{\rho_{Blend} - \rho^{(A)}_{Blend}}{\rho^{(C)}_{Blend} - \rho^{(A)}_{Blend}} \times \frac{\rho^{(C)}_{Blend}}{\rho_{Blend}} \times 100$$

ρ_{Blend} = Density of a given composition of the blend fiber found experimentally.

It is seen from Figure 11 that the crystallinity increases steadily up to 60/40 nylon 6/PET composition after which it decreases for the 50/50 fiber composition. This shows that addition of PET to nylon 6 and consequent fiber formation leads to an increase in the order in the structure of the blend fiber system. This is also borne out by the reinforcement of the (202, 002) lattice planes as observed from X-ray studies. The trend observed in the two cases is same. Thus the increase in the PET content after a certain limit seems

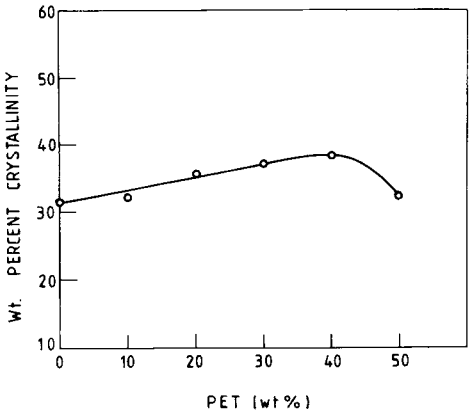

Fig. 11. Composition dependence of density crystallinity in nylon 6/PET blend fibers.

to distort the nylon 6 crystalline domains giving rise to a reduction in density crystallinity as also to reduced (202, 002) reflection of nylon 6 at 60/40 nylon 6/PET or high PET content.

Both heat of fusion crystallinity and density crystallinity show good agreement with a slight difference of optimum composition corresponding to highest crystallization of nylon 6 in the blend. These results suggest that when PET is blended into nylon 6 it is mainly the nylon 6 constituent which crystallizes. This may be due to highly oriented PET chains acting as nuclei for the formation of nylon 6 crystals. When PET content becomes comparable to that of nylon 6 no further formation of nylon 6 crystals may be possible when maximum nucleation has already occurred. Even amorphous polymers have been reported to affect crystallization in blends by the constraints they impose. In his studies of nylon 6/nylon 11 and nylon 66/nylon 6 blends Inoue[11] reports that the major component in the blend crystallizes to a higher degree than the minor component, and thus crystalline polymers may serve as nucleation substrates for crystallizing polymers and thereby affect crystallization kinetics, morphology, and level of final crystallinity. Papero et al.[12] have observed that in the case of nylon 6/PET blend fibers the major constituent appears to crystallize to a higher degree than the minor constituent.

From the DSC and DTA of the blend fibers it is seen that nylon 6 and PET melt at their respective melting temperatures (Figure 8). There is no lowering of the melting points of nylon 6 meaning thereby that under the conditions employed for melt blending nylon 6 and PET and consequent spinning of the blend no transesterification has occurred. Kitao et al.[13] hold that if a blend has a more microhomogeneous structure the melting behavior of the component of higher T_m is probably affected by the molten component of lower T_m. Thus, we say that our nylon 6/PET blend fiber system is not a microhomogeneous system and whatever improvement in properties is achieved is due to the fibril-reinforced composite morphology developed in it and the crystallization of the two components, especially that of nylon 6 component. There is no chemical interaction between the two constituents and the property enhancements are due to the ability of the constituent materials to remain in molecular contact when constraints are imposed on the structure.

The crystallization exotherm for the blends occurs around 116°C, while that of PET is seen to be around 136°C. This corresponds to the crystallization of PET since this crystallization peak is missing for nylon 6. The lowering of the crystallization peak of PET when present in the blend suggests that nylon 6 is aiding in the crystallization of PET. Thus, nylon 6 and PET in the blend may be aiding each other in mutual nucleation with nylon 6 crystallizing to a higher degree than PET.

CONCLUSIONS

In the nylon 6/PET blend system PET is dispersed as spheres which on drawing becomes rodlike and thus a fibril matrix type morphology is developed. The increase in the crystallinity of nylon 6 in the blend fiber is due to PET reinforcing the (202, 002) lattice planes of nylon 6. The initial increase in crystallinity of nylon 6 is due to the highly oriented PET chains acting as nuclei for the formation of nylon 6 crystals. When PET content exceeds 30–40%, the nylon 6 crystalline domains get distorted. The increased orientation of the blend fiber is due to highly oriented and extended PET chains holding the nylon 6 molecular chains along their length. The blend system is essentially incompatible. The improvement in properties is achieved due to the fibril-reinforced morphology and the crystallization behavior of the two components, especially that of nylon 6 in the presence of PET.

References

1. L. E. Alexander, *X-ray Diffraction Methods in Polymer Science*, Wiley Interscience, John Wiley and Sons, Inc., New York, 1969.
2. M. I. Pope and M. D. Judd, *Differential Thermal Analysis*, Heyden and Son Ltd., London, 1977.
3. M. Inoue, *J. Polym. Sci.*, **A1**, 2697 (1963).
4. J. Brandrup and E. H. Imergut, *Polymer Handbook*, Wiley Interscience, New York, 1975.
5. L. H. Sperling, *Recent Advances in Polymer Blends, Grafts and Blocks*, Plenum, New York, 1974.
6. J. Shimizu, N. Okui, T. Yamamoto, M. Ishii, and A. Takaku, *Sen-I Gakkaishi*, **38** (4), T-153, (1982).
7. B. B. Stafford, *J. Appl. Polym. Sci.*, **9**, 729 (1965).
8. N. V. Mikhailov, E. Z. Fainberg, V. O. Gorbacheva, and Chen Tsin-Khai, *Polym. Sci. USSR*, **4**, 83 (1963).
9. A. Wlochowicz and A. Jeziorny, *J. Polym. Sci. Polym. Chem. Ed.*, **11**, 2719 (1973).
10. B. Wunderlich, *Macromolecular Physics* Vol. 1, Academic Press, New York, 1973.
11. M. Inoue, *J. Polym. Sci.*, **A-1**, 3427 (1963).
12. P. V. Papero, E. Kubu, and L. Roldan, *Text. Res. J.*, **37**, 823 (1967).
13. T. Kitao, H. Kobayashi, S. Ikegami, and S. Ohya, *J. Polym. Sci. Polym. Chem. Ed.*, **11**, 2633 (1973).

Received September 19, 1985
Accepted October 1, 1985